Comprehensive Residual Stress Distributions in a Range of Plate and Pipe Components

Hyeong-Yeon Lee*, Jong-Bum Kim, Jae-Han Lee
Member, Mechanical Engineering Division, Korea Atomic Energy Research Institute, Dukjindong 150, Yuseong 305-353, Korea
Kamran M. Nikbin
Department of Mechanical Engineering, Imperial College London, South Kensington Campus, London, SW7 2AZ, United Kingdom

A comprehensive review of through thickness transverse residual stress distributions in a range of as-welded and mechanically bent components made up of a range of steels has been carried out, and simplified generic transverse residual stress profiles for a plate and pipe components have been proposed. The geometries consisted of welded pipe butt joints, T-plate joints, tubular T-joints, tubular Y-joints and a pipe on plate joints as well as cold bent tubes and pipes. The collected data covered a range of engineering steels including ferritic, austenitic, C-Mn and Cr-Mo steels. Measured residual stress data, normalised with respect to the parent material yield stress, has shown a good linear correlation versus the normalised depth of the region containing the residual stress resulting from the welding or cold-bending process. The proposed simplified generic residual stress profiles based on the mean statistical linear fit of all the data provides a reasonably conservative prediction of the stress intensity factors. Whereas the profiles for the assessment procedures are fixed and case specific, the simple bilinear profiles for the residual stresses obtained by shifting the mean and bending stress from the mean regression line have been proposed and validated.

Key Words : Residual Stress, As-Welded, Stress Intensity Factor, T-Plate, Tubular T-Joint

1. Introduction

The detrimental effect of a residual stress on a structural integrity needs to be addressed in failure assessments. Residual stresses are introduced, to varying degrees, by almost all manufacturing processes although their adverse effects are particularly apparent in welded joints. When components are joined together by a fusion welding, due to the high temperature gradients and plastic deformations near the weld, residual stress fields are set up in the vicinity of the welded joint. It is important that such stresses are accounted for in safety assessment procedures such as the UK structural integrity procedures, R6 (British Energy, 2001) and BS7910 (British Standard, 2000). Since information is often not directly available on the residual stress distributions, compendia with recommended (upper-bound) residual stress profiles for use in structural integrity analyses are included in R6 and BS7910.

In this study, the residual stress distributions typical of those due to a welding and fabrication process were reviewed and the representative distributions for a range of weld joint types were examined. Stress profiles have been collated from data available in the public domain for various types of weld geometries (Bate et al., 1995). The

* Corresponding Author,
E-mail : hylee@kaeri.re.kr
TEL : +82-42-868-2956; **FAX** : +82-42-861-7697
Member, Mechanical Engineering Division, Korea Atomic Energy Research Institute, Dukjindong 150, Yuseong 305-353, Korea. (Manuscript **Received** August 26, 2005; **Revised** January 28, 2006)

weld geometries covered in this work are a pipe butt, pipe on plate, tubular Y-joint, tubular T-joint and T-plate. Fabrication induced residual stresses due to a cold bending of pipes (Kwon et al., 2001) were also examined in this study ; due to the inhomogeneous plastic deformation during a bending, a residual stress distribution is established in a pipe. The measured data covers a range of conditions such as materials, measurement methods, weld heat input, weld geometries and boundary restraints. The materials included in the present geometries are ferritic, austenitic, C-Mn and Cr-Mo steels. The measurement methods used include a neutron diffraction, X-ray diffraction, hole drilling and sectioning and a block removal.

Linear elastic stress intensity factors (SIFs) have been determined by using a superposition method (Wu and Carlsson, 1995 ; Lee et al., 2005a) in conjunction with a finite element analysis. The results were compared with the SIFs obtained by using the stress distribution recommended in the assessment procedures R6 and BS7910. Note that the validity range of the yield strength, thickness and electrical heat input for the welded joints in R6 is somewhat restricted and some of the distributions presented are outside these limits. Assessment of a fatigue, fracture or creep-fatigue damage for a welded structure has been carried out (Lee et al., 1998 ; 2003 ; 2004 ; 2005b) without a quantitative estimation of the residual stresses.

In a previous work, the recommended residual stress distributions in R6 and BS7910 were shown to be conservative (O'Dowd et al., 2004 ; Lee et al., 2005a ; Wimpory et al., 2003). In this work comprehensive representative residual stress distributions for a range of geometries, materials and fabrication processes were examined.

2. Material Specifications and Geometries

T-plate specimens were fabricated with high strength ferritic steel (designated SE702, equivalent to the A517 Grade Q steel) and medium strength low carbon ferritic steel, BS EN 10025 S355 (British Standard, 1993). The tubular T-joint was manufactured from BS 7191 Grade 355 EMZ (British Standard, 1989). The specific material properties and weld parameters for the weld geometries are provided in Tables 1 and 2, respectively. Manual metal arc (MMA) welding was performed to manufacture the T-plate and tubular T-joint samples.

The dimensions of the welded T-plate and the tubular T-joint are provided in Figs. 1 and 2, respectively. A fracture assessment was carried out for the above two geometries. Besides the above two weld geometries, the other geometries shown in Fig. 3 — pipe butt welds, tubular Y-joint and pipe-on-plates — were collected from the literature to build up comprehensive residual stress profile.

Table 1 Specific uniaxial tensile properties

Material	σ_y (MPa)	σ_u (MPa)	E (GPa)
BS EN 10025 GradeS355	348	515	212
SE 702	700	790-940	205
BS 7191 Grade 355 EMZ	355	460-620	—

Table 2 Weld parameters

Geometry	Material	Weld passes	Current (A)	Voltage (V)	Heat Input (KJ/mm)
T-plate	BS EN 10025 S355	18	170-240	21-23	2.0~2.5
	SE702	25	160	22	1~2
Tubular T-joint	BS7191 Grade 355	30	500-560	30-31	3.6

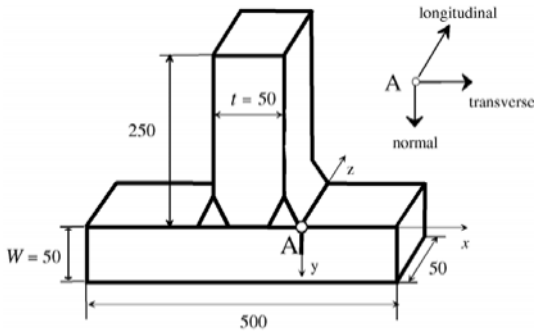

Fig. 1 Geometry of the T-plate (SE702), all the dimensions are in mm (not to scale)

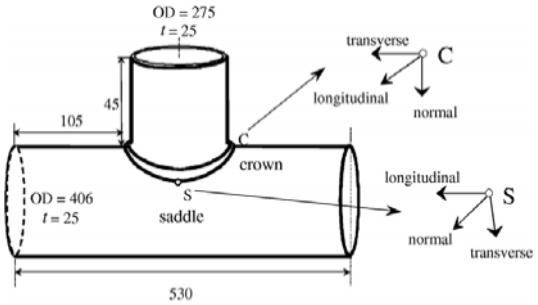

Fig. 2 Geometry of the tubular T-joint, all the dimensions are in mm (not to scale)

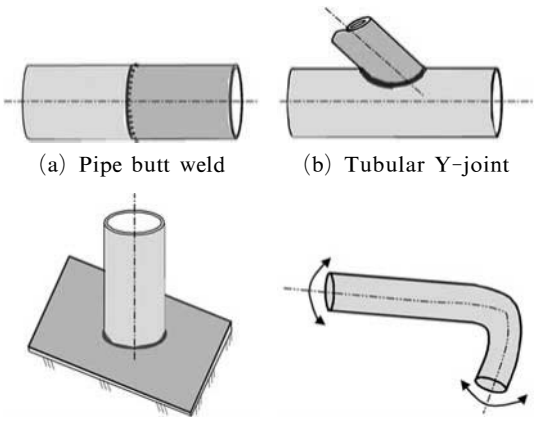

(a) Pipe butt weld (b) Tubular Y-joint

(c) Pipe on plate (d) Bent pipe

Fig. 3 Schematic diagrams of the additional geometries analysed

3. Measured Residual Stress Distributions

Data from the geometries described has been compared and presented in Fig. 4. The transverse

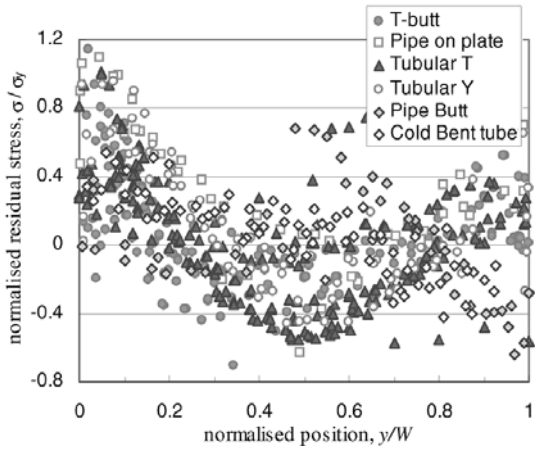

Fig. 4 Transverse residual stress distribution for a range of welded joint types

residual stresses for a range of geometries and materials normailised with their respective yield stresses are included in Fig. 4. It can be seen that when the measured data is considered for up to $y/W=0.5$ (half of specimen thickness), the stress distributions are represented well by using a straight line as shown in Fig. 5. The region of interest for a life assessment is the short crack region starting at the surface and therefore $y/W=0.5$ is usually well beyond the safety margin that is considered in an actual application. The measuring methods of the residual stresses induced by a welding or mechanical bending for a range of geometries as well as weld details are shown in Table 3. Neutron diffraction measurements were carried out to measure the stresses along a line at the weld toe through the plate (y-direction in Fig. 1) for the T-plate. Also the neutron diffraction method was used to measure the residual stresses at the locations of the crown and saddle as shown in Fig. 2. The three normal stress components of normal, transverse and longitudinal as indicated in Figs. 1 and 2 have been measured. Neutron diffraction methods for measuring the residual stress can be used to determine non-destructively the stress state inside a sample, by measuring the changes in the lattice spacing from the 'un-stressed' states. Neutrons have a penetration depth of several cm in most metals, allowing the deep stress state inside a

Table 3 Measurement of the residual stresses and the weld details

Geometries	Measurement method	Plate thickness (mm)	pass	Yield stress (MPa)	Heat input (KJ/mm)
T-Butt	Neutron Diffraction	50 50	18 25	348 700	1~2 2~2.5
Pipe on plate (Porter Goff, 1998)	Hole Drilling & Sectioning	22	7	420	1.41
Tubular T	Neutron Diffraction	25	30	355	3.6
Tubular Y (Porter Goff, 1989)	Block Removal	22	6	430	1.8
Pipe Butt (Scaramangas, 1985)	Sectioning & hole drilling & EDM	9.1	—	520	0.8
Cold Bent Tube (Kwon et al, 2001)	X-ray Diffraction	31	N/A	—	N/A

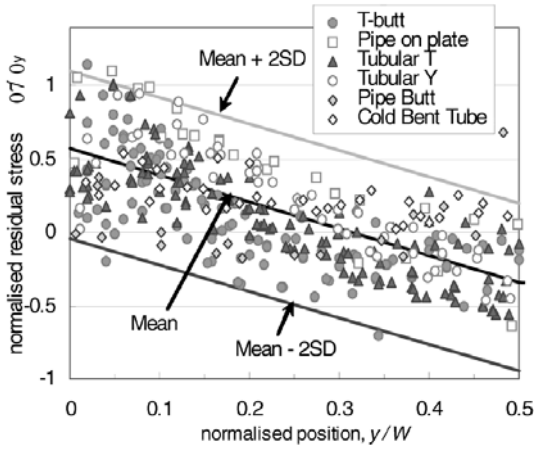

Fig. 5 Transverse residual stresses for a range of welded geometries including the mean, and the upper and lower bounds of the data

sample to be determined (O'Dowd et al., 2004). In this study, it is intended to propose a comprehensive residual stress profile covering all the cases in Fig. 5 over the crack ratio up to half the thickness ($a/W \leq 0.5$) based on the statistical analysis to be explained in the following section.

4. Statistical Analysis

The measured data in Fig. 5 is the first half part of Fig. 4 which covers the region of $y/W \leq 0.5$. It can be seen that all the normalised residual stress data (σ/σ_y) can be conveniently described by a linear regression line which contains a wide scatter. The variability of the data can be attributed to the differences in the geometry and materials as well as to a great extent to the scatter in the measurements of the residual stresses which in some cases could be as much as $\pm 30\%$. Given the wide variability, it would therefore be feasible to simplify the data to a linear relationship as shown in Fig. 5 and to treat the data statistically. Table 3 shows the individual linear regression lines of the transverse stresses up to $y/W=0.5$ for all the considered cases. Least square linear fits have been calculated for each of the data sets individually as well as for all the data and they are shown in Table 3. However, as shown in Fig. 4, the overall magnitudes of the stresses irrespective of the component, material and type of residual stresses are comparable once the stresses are normalised by the yield strength.

Figure 5 shows the best fit mean values for all the data and the upper/lower bound lines at two standard deviations (2SD). The corresponding values of the mean slopes and standard deviations for the datasets are provided in Table 4. The analysis of the individual data sets shows that the pipe-butt has the lowest mean slope and the pipe-on-plate has the highest slope. The standard deviation meaning the degree of the scatter from the mean is relatively high for the pipe-on-plate, tubular Y and the tubular T. The present analysis by using the data in Fig. 5 is based on the 'mean$\pm$2SD' and 95% of the distribution will

Table 4 Analysis of the residual stress data

	Case	Linear Regression Line	Standard Deviation (SD)
Welds	T-butt	$-1.852x+0.485$	0.361
	Tubular T	$-2.001x+0.563$	0.373
	Tubular Y	$-2.261x+0.791$	0.386
	Pipe Butt	$+0.197x-0.006$	0.235
	Pipe on plate	$-2.626x+1.020$	0.451
Mech. Forming	Cold bent tube	$-0.634x+0.399$	0.135
All	All	$-1.755x+0.551$	0.260

be inside the band. If the band is expanded to 'mean±3SD' in order to take the high level of reliability that is required into account, 99.7% of the distribution will be located inside the band. Therefore, a linear fit with higher SD values (e.g '±3SD') can be used rather than employing the complicated non-linear curve fitting for the mean data. The normalized linear mean line, for all the data, shown in Fig. 5 is given by:

$$\hat{\sigma}=-1.755x+0.551 \tag{1}$$

where $\hat{\sigma}=\sigma/\sigma_y$ and $x=y/W$.

The form of Eq. (1) indicates that the normalised mean curve is composed of a membrane (uniform) stress component of approx. 0.55 and a bending (linear) stress with a slope of approx. −1.76. The degree of conservatism in estimating the SIF for the T-plate and tubular T-joint geometries, using a linear fit of this type, has been examined in a previous work (Lee et al., 2005a).

5. Residual Stress Profiles from the R6 and BS 7910 Procedures

5.1 R6 distributions for a T-plate and a tubular T-joint

In the R6 procedure, two approaches for defining the transverse residual stress profiles in welded T-plates are provided, depending on the available information about the welding conditions. If the welding conditions are known or can be estimated, then the residual stress profiles given by the following Eqs. (2) and (3) may be used, which are associated with the size of the plastic zone (r_o). If the welding conditions are unknown, polynomial functions are provided.

The recommended through-thickness transverse residual stress distribution in the T-plate consists of an upper bound bilinear profile. The peak stress is at the weld toe and equal to the parent material yield stress and it reduces linearly to zero at a distance r_o from the weld toe. An initial estimate for r_o is given by,

$$r_o=\sqrt{\frac{K}{\sigma_y}\frac{\eta q}{\nu}} \tag{2}$$

where K is a material constant that depends on the coefficients of a thermal expansion, Young's modulus, a density and specific heat of a material (Nmm/J), σ_y is the yield or a 0.2% proof strength of the parent metal, q is the arc power, ν is the weld travel speed and η is the process efficiency (fraction of arc power entering plate as heat). Typical values of K and η for a range of materials are provided in the procedures. For ferritic steels the values provided are $K=153$ Nmm/J and $\eta=0.8$.

If Eq. (2) results in a plastic zone greater than the plate width ($r_0>W$), r_0 must be recalculated by using,

$$r_o=\frac{1.033K}{\sigma_y}\frac{\eta q}{\nu(W+0.5t)} \tag{3}$$

The value of r_0 obtained from Eq. (2) for both T-plate geometries analysed here, gives $r_0=25$ mm for the SE702 and $r_0=27$ mm for the Grade S355 steel. Since these two values are very close, a single R6 curve is plotted in Fig. 6 with $r_0=26$ mm.

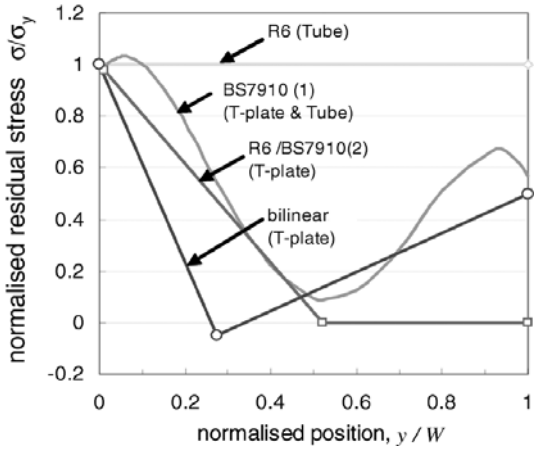

Fig. 6 Recommended residual stress distributions for the T-plate and the tubular T-joint

The Tubular T-joint is included in the 'Pipe T-butt weld' section of the R6 procedure. The profiles are generated from geometries where the ratio of the chord thickness (main pipe) to the brace thickness (branch pipe) varies from 1.375 to 2. For cases where $W/t<1.375$, a uniform tensile residual stress is assumed. For cases were $W/t>2$, the profiles of the above plate T-butt welds are recommended. For cases were $1.375<W/t<2$, the same equation as in BS7910 is applied (see below). In the present tubular T-joint with $W/t=1$, the recommended R6 distribution is a uniform stress of the yield stress magnitude through the thickness, as shown in Fig. 6.

5.2 BS 7910 distributions for a T-plate and a tubular T-joint

BS7910 provides two transverse residual stress distributions for T-plate joints. The first transverse residual stress distribution is a polynomial function representing an upper bound fit to experimental data and it is given by the following Eq. (4). This distribution is referred to as BS7910 (1) in this paper.

$$\hat{\sigma}=0.97+2.3267x-24.125x^2+42.825x^3-21.087x^4 \quad (4)$$

where $\hat{\sigma}=\sigma/\sigma_y$ and $x=y/W$ as in Eq. (1).

The second distribution in BS7910 follows that in R6, with the distribution dependent on the size of the plastic zone. When the plastic zone size r_o calculated by Eq. (2) is less than the base plate thickness, the residual stress is taken to be that of the parent material yield stress at the weld toe, reducing linearly to zero over the size of the yielded zone as in R6. However, Eq. (3) is not used in BS7910. If Eq. (2) results in a plastic zone greater than the base plate width, the stress is taken to be equal to the yield strength across the whole specimen thickness. This distribution is referred to as BS 7910 (2) in this paper.

The recommended BS7910 transverse residual stress profile for the tubular T-joint is the same polynomial function as that provided for T-plate welds (Eq. (4)). The distribution is provided in Fig. 6. It should be noted that for the current geometry, BS7910 provides a more conservative residual stress profile than R6 for the T-plate while R6 is more conservative for the tubular T-joint.

5.3 Bilinear distribution

A bilinear distribution has been proposed recently (Wimpory, 2003), based on residual stress data for a range of T-plate joints in ferritic steels. This distribution, which has been obtained by shifting an approximate mean bilinear fit to the data by a uniform (membrane) stress of $0.25\sigma_y$, is shown in Fig. 6. It can be seen that for the available stress distributions for a T-plate, the polynomial function distribution of BS7910 (1) is the most conservative followed by the R6 distribution and then the bilinear distribution for a T-plate.

6. Finite Element Analysis

The stress intensity factors have been determined by using a finite element (FE) analysis in conjunction with the superposition method (O'Dowd, 2004; Lee, 2005). A total of 13,540 linear elements and 14,094 nodes have been used; the smallest element size is 0.03 mm ($6\times10^{-4}W$) for the T-plate mesh as shown in Fig. 7(a). The tubular joint is a three dimensional geometry, but here it is represented by an axisymmetric, "tube on plate" FE mesh as shown in Fig. 7(b). A total of 13,534 linear elements and 14,091 nodes were

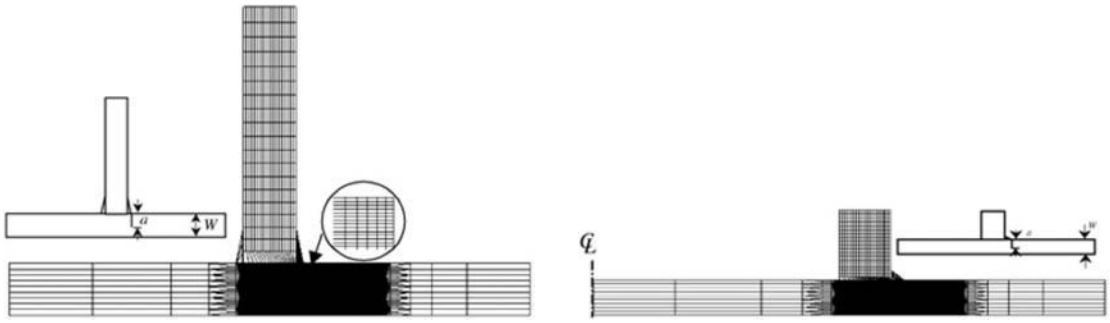

(a) (b)

Fig. 7 Finite Element Meshes (a) T-plate (b) Representation of the tubular T- joint

used and the smallest element size is 0.015 mm ($6\times10^{-4}W$). Such a fine mesh was used for the two geometries rather than using a focused mesh near the crack tip because it is easier to model different crack lengths ($0<a/W\leq0.5$) with a conventional fine mesh. The crack is modelled along the thickness direction as shown in Fig. 7 (a) and 7(b). The FE models with a specific crack length (a/W) of 0.1, 0.2, 0.3, 0.4 and 0.5 were used for the calculation of the SIFs. All the finite element analyses were carried out by using the commercial FE software package, ABAQUS 6.4 (2004).

Only the crack surface stresses need to be considered for the loading condition in the calculation of the SIF based on the superposition principle, and only transverse residual stresses were considered for the calculation of the mode I SIFs.

7. Results of the Analysis

7.1 Sensitivity analysis with linear regression lines

As shown in Fig. 8 the present residual stress profiles are case specific and based on a shift in the membrane stress above the upperbound of the measured data. However it is possible to define a generic stress profile (normalised using the lowerbound yield stress) in terms of a linear shift in the mean line of the data and/or a shift in the bending stress based on the statistical data of all the data shown in Fig. 5. A sensitivity analysis of the SIFs by using changes in the

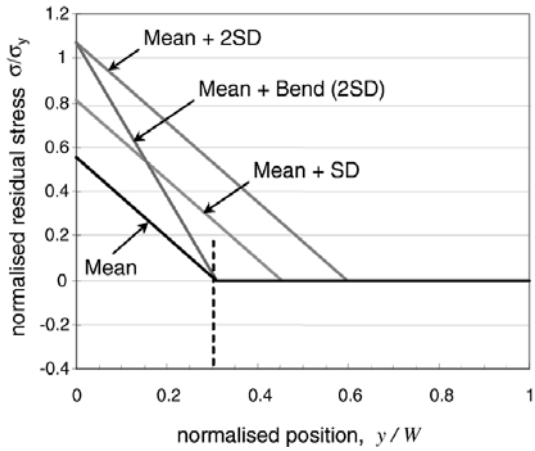

Fig. 8 Definition of the Mean + bend lines

membrane and bending stresses with respect to the average linear fit of Eq. (1) was conducted. Shifting the mean line by one, two or three standard deviations corresponds to the addition of a membrane stresses of one, or two or three SDs (standard deviations), respectively. The magnitude of this shift can be chosen according to the required degree of reliability or conservatism for the problem being considered. In addition any negative stress distribution across the section is taken as zero for a further conservatism. This type of approach is useful because there is usually some degree of scatter due to an uncertainty in the measurements and a lack of experimental data. The linear fits of a 'mean+SD', 'mean+2SD' and a 'mean+bend (2SD) at the surface' were carried out. The first two lines are obtained by considering a shift of the membrane stresses from the

mean regression line of Eq. (1). The third line is obtained by shifting the mean stress at the surface by 2SD to increase the bending. In all the cases any line in the compressive region is assumed to give a zero stress for an added conservatism for longer crack lengths.

The first distribution line to be considered as a potential 'comprehensive residual stress distribution' is the 'mean+SD' line which is the mean line shifted by one standard deviation (SD) (0.26 σ_y in Table 3) and 68.3% of the data points are located below this line. The equation for this line is

$$\hat{\sigma} = -1.755x + 0.811 \quad (5)$$

The second 'comprehensive residual stress distribution' is 'mean+2SD' and more than 95% of the data would be located within this band of the 'mean±SD' line. The 'mean+2SD' line is represented by

$$\hat{\sigma} = -1.755x + 1.071 \quad (6)$$

If a higher reliability is required, the band can be expanded to 'mean+3SD' (99.7%) or even further.

A third potential 'comprehensive residual stress distribution' is the one obtained from Eq. (1) with the pivot point fixed at $y/W=0.31$ which is the intercept point of the mean line with the x-axis. A bending stress of $0.52\sigma_y$ (2SD) is added to the mean line to give a 'mean+bend' line. The stress beyond the pivot point is set to zero for a conservatism. Case studies of changing the bending stress rather than the membrane stress have been examined in a previous work (Lee, 2005a) and it was shown that changing the bending stress is a promising approach for determining less conservative residual stress distributions. In this context, the mean line was adjusted to include a bending term and only the tensile area was considered as a comprehensive stress distribution. Then the stress distribution becomes

$$\begin{aligned} \hat{\sigma} &= -3.456x + 1.071 \quad \text{for } x < 0.3 \\ &= 0 \qquad\qquad\qquad\quad \text{for } x \geq 0.3 \end{aligned} \quad (7)$$

Since all the details of the geometry and materials for the different weld data presented in Fig, 5 are not available, fracture assessments for the residual stress distributions of Eqs. (5)-(7) were carried out, only for the T-plate and tubular T-joint.

7.2 Stress Intensity Factors (SIFs) for T-plates

The SIFs for the R6 and BS7910 distributions of Fig. 6 and the three potential stress distributions of Fig. 8 are shown in Fig. 9. The figure shows that the SIFs from the BS7910 distribution and the 'mean+2SD' are almost identical and the most conservative. And the R6 line, the 'mean+bend' line and 'mean+SD' line follow in terms of a conservatism. In Fig. 9, the SIFs obtained using the data from the Grade S355 T-plate are compared with the other five distributions. It can be seen that the 'mean+SD' and 'mean+bend' lines provide good results. The 'mean+SD' line is less conservative for short cracks ($a/W<0.3$) while the 'mean+bend' is less conservative for long cracks ($a/W \geq 0.3$). It should be noted that the 'mean+SD' and 'mean+bend' lines give better results than the R6 and BS7910 lines although they were derived from the dataset shown in Fig. 5, covering a range of weld geometries.

7.3 Stress intensity factors for the tubular T-joints

The results for the SIFs obtained using the recommended distributions of R6, BS7910, the

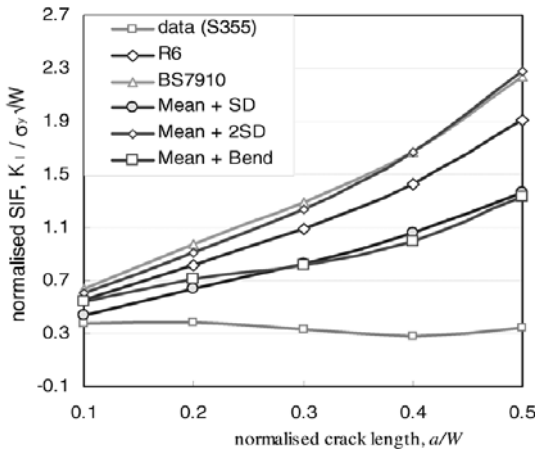

Fig. 9 Stress intensity factors for the T-plate

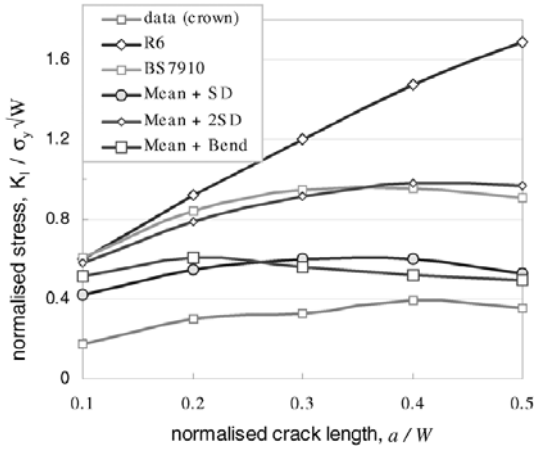

Fig. 10 Stress intensity factors for the tubular T-joint

'mean+SD' and 'mean+2SD' lines are shown in Fig. 10 for the tubular T-joint. The results were obtained for the distributions of Figs. 6 and 8 for the tubular T-joint. Fig. 10 shows that the R6 distribution is the most conservative and the BS7910 and 'mean+2SD' are again almost identical

It should be noted that these two profiles of 'mean+SD' and 'mean+bend' for the tubular T-joint give better results than the R6 and BS7910 distributions. For the tubular T-joint, the behaviour of the 'mean+SD' and the 'mean+bend' lines are very similar as is the case in the T-plate although the 'mean+SD' line is less conservative for short cracks ($a/W \leq 0.2$) while the 'mean+bend' line is less conservative for long cracks ($a/W \geq 0.3$).

As promising comprehensive residual stress distributions, Figs. 9 and 10 show that the two linear lines of 'mean+SD' and 'mean+bend' are appropriate for the distribution of transverse residual stresses, covering a range of weld geometries and materials with less conservatism than the existing procedures of R6 and BS7910.

8. Conclusions

In this study, a review of the residual stress distributions for a range of welded joint types as well as cold bend tubes consisting of a range of steels has been carried out. Based on the experimentally measured data of the wide range of components considered, a set of comprehensive transverse linear residual stress profiles (derived from the residual stresses normalised with yield stress) has been proposed which give reasonably conservative estimates for a calculation of the linear elastic stress intensity factors across the thickness of the range of components investigated. The SIF estimates using the present profiles for the T-Plate and tubular T-joint geometries are shown to be less conservative when using the residual stress distribution profiles from the current procedures (R6, BS7910).

Calculation of the SIF by using the linear profile showed that the residual stress profile of 'mean+bend' and 'mean+SD' gave less conservative values with a reasonable conservatism both for the T-plate and the tubular T-joint. It was also shown that the SIFs due to 'mean+2SD' were very similar to those of BS7910 for both the T-plate and the tubular T-joints. The adjustment of the mean shift which means increasing the membrane stress by some multiple of the standard deviation with and without an adjustment of the slope depends on the degree of the reliability required in the calculation. Whereas the recommended residual stress distributions are geometrical and material specific, it is shown that a simplified comprehensive linear profile (normalised with the material yield stress) can provide sufficiently conservative guidelines for a wide range of components and materials which are likely to have tensile residual stress distributions resulting from either a welding or a mechanical bending. For an added conservatism where there are compressive residual stresses present, the profile distribution is assumed to be at a zero stress. The use of this generic linear model is appropriate in the cases where there is insufficient information on the weld procedures or residual stress profiles.

Acknowledgments

This study was supported by the Korean Ministry of Science & Technology through its National Nuclear Technology Program.

References

Bate, S., Green, D. and Buttle, D., 1995, "A Review of Residual Stress Distributions in Welded Joints for the Defect Assessment of Offshore Structures," AEA Technology, OTH95-482.

British Energy Generation Ltd, 2001, *Assessment of the Integrity of Structures Containing Defects*, R6 Rev. 4. British Energy Generation Ltd, UK.

British Standard Institution, 2000, *Guide on methods for assessing the acceptability of flaws in metallic structures*, BS7910 : 1999 (Rev. March 2000) British Standards Institution, London, UK.

British Standard Institution, 1993, *Hot rolled products of non-alloy structural steels — technical delivery conditions*, BS EN 10025 : 1993.

British Standard Institution, 1989, *Weldable structural steels for fixed offshore steels*, BS 7191 : 1989.

Hibbitt, Karlsson and Sorensen Ltd. 2004, ABAQUS, *version 6.4*.

Kwon, O., Pathiraj, B. and Nikbin, K. M., 2001, "Effects of Residual Stress in Creep Crack Growth Analysis of Cold Bent Tubes Under Internal Pressure," *International Journal of Pressure Vessel and Piping* (*IJPVP*), Vol. 78, pp.343～350.

Lee, H. -Y., Kim, J. -B. and Lee, J. -H., 2003, "Progressive Inelastic Deformation Characteristics of Cylindrical Structure with Plate-to-shell Junction Under Moving Temperature Front," *Korean Society of Mechanical Engineering* (*KSME*) International Journal, Vol. 17, No. 3, pp. 403～411.

Lee, H. -Y., Biglari, F., Wimpory, R., O'Dowd, N. P. and Nikbin, K. M., 2005a, "Treatment of Residual Stresses in Life Assessment Procedures," *Submitted to Engineering Fracture Mechanics*, August.

Lee, H. -Y., Kim, J. -B., Kim, S. H., Park, C. -K. and Lee, J. -H., 2005b, "Creep-Fatigue Damage Evaluation for a Welded Cylindrical Shell with Defects," ICAPP 2005, ANS, Seoul, Session 8.02.

Lee, H. -Y., Kim, J. -B. and Lee, J. -H., 2004, "Evaluation of Progressive Inelastic Deformation for the Welded Structure Induced by Spatial Variation of Temperature," *IJPVP*, Vol. 81. No. 5, pp. 433～441.

Lee, H. -Y., Kim, J. -B. and Yoo, B., 1998, "Damage Evaluation of 304 and 316LN Stainless Steel Structure with Prior Damage Under Creep-fatigue Loading," *KSME*, Vol. 22, No. 12, pp. 2269～2277.

May, P., 2002, *Effect of welding residual stresses on the fracture resistance of ductile steels*, Ph.D. Thesis, Imperial College London.

O'Dowd, N. P., Nikbin, K. M., Lee, H. -Y., Wimpory, R. and Biglari, F., 2004, "Stress Intensity Factors Due to Residual Stresses in T-plate Welds," *Journal of Pressure Vessel Technology*, ASME, Vol. 126, pp. 432～438.

Wimpory, R., May, P., O'Dowd, N. P. Webster, G., Smith, D. and Kinston, E., 2003, "Measurement of Residual Stresses in T-Plate Weldments," *Journal of Strain Analysis*, 38 (4), pp. 3469～365.

Wu, X. and Carlsson, A., 1991, *Weight Functions and Stress Intensity Factors Solutions*, Pergamon Press.